Contribution to Structural Mechanics of Patch-Based Composites

Andreas Baumer, André Baeten

Augsburg University of Applied Sciences
Faculty of Mechanical and Process Engineering

An der Hochschule 1, 86161 Augsburg, Germany

Hochschule Augsburg
University of Applied Sciences

1 Introduction - Fiber Patch Placement

Fiber Patch Placement (FPP) sets a new milestone in manufacturing of high-performance composite structures, as it enables fully-automated processing of fiber-reinforced plastics with defined variable fiber orientation. This qualifies FPP for a wide range of applications in high-tech industries such as aerospace, automotive or medical technology.

First, MEYER developed the basic manufacturing process and created first design guidelines for patched laminates. [2] The Cevotec GmbH further developed the process, raised it to a high maturity level (see Figure 1) and has started selling the system in different configurations. Experimental investigations and FEA simulations of various FPP laminate design parameters (patch-length, patch-thickness, overlap pattern) were conducted by HORN and KUSSMAUL. [3], [4]

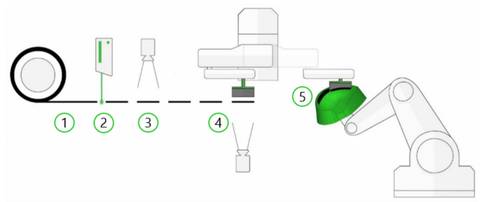

Figure 1: Schematic illustration of the FPP process: (1) feeding of fiber tape, (2) (laser-)cutting of tape in patches, (3) inspection of patches, (4) picking up and position check of patches, (5) placing the patches onto the forming tool. [1]

The structural mechanical considerations in this work aim to deliver an analytical description for the elasticity parameters of a FPP lamina to explain the experimentally determined laminate stiffness and strength.

2 Engineering Constants of an FPP lamina

Patch-based laminates have a significantly different fiber architecture compared to classic laminates with continuous plies. For the determination of the moduli of elasticity one individual structural FPP lamina is considered (see Figure 2) and following assumptions are made: [2]

- unidirectional fiber orientation along x-axis,
- constant patch thickness,
- patch length and overlap $\geq$ crit. fiber length ($l_{critical} \approx 1,000$x filament-$\varnothing$; $l_{critical,CFRP} \approx 5$ mm),
- patch pattern with negligible gaps (resin pockets) at butt joints,
- neglecting of bending moments or stress concentrations at fiber ends.

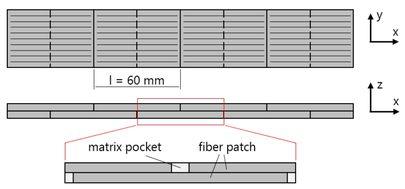

Figure 2: Structural FPP lamina with representative unit cell.

SCHÜRMANN's micro-mechanical elastic spring models are applied on a meso-mechanical scale: Creation of a representative meso-mechanical model, selection of an appropriate spring model (parallel or series connection), determination of engineering constants with an elasto-static approach (system of equations of equilibrium of forces, kinematic relations and law of elasticity). [5]

2.1 Longitudinal Young's Modulus $E_\parallel$

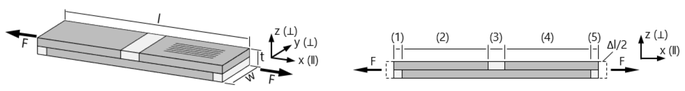

Figure 3: Representative unit cell of FPP lamina with uniaxial loading in fiber direction.

In section (2) and (4) the Young's modulus corresponds to that of the patch material (continuous reinforced composite): $E_{(2)} = E_{(4)} = E_{patch}$. The Young's modulus in the butt joint sections (1), (3) and (5) is the arithmetic mean of the patch and matrix material: $E_{(1)} = E_{(3)} = E_{(5)} = (E_{patch} + E_{matrix})/2$. The modulus of elasticity of the FPP unit cell is obtained by serial connection of the sections:

Equilibrium of forces: $F_\parallel = F_i$ or $\sigma_\parallel = \sigma_i$; $i = (1), (2), (3), (4), (5)$

Kinematic relations: $\Delta l_\parallel = \Sigma \Delta l_i$; $\Delta l_i = \varepsilon_i \cdot l_i \Rightarrow \varepsilon_\parallel \cdot l_\parallel = \Sigma \varepsilon_i \cdot l_i$

Law of elasticity: $\varepsilon_i = \frac{\sigma_i}{E_i}$; $\frac{\sigma_\parallel}{E_\parallel} = \Sigma \frac{\sigma_i}{E_i} \cdot l_i \Rightarrow \frac{1}{E_\parallel} = \Sigma \frac{1}{E_i} \cdot l_i$

Assumptions made: $\frac{l_{(2)}+l_{(4)}}{l_\parallel} \approx 1$ (patch sections) ; $\frac{l_{(1)}}{l_\parallel} = \frac{l_{(3)}}{l_\parallel} = \frac{l_{(5)}}{l_\parallel} \approx 0$ (butt joint sections)

$\Rightarrow$ Patch-based fiber architecture shows the same stiffness in fiber direction as endless-reinforced composite material. This was proven by experiments in the work of HORN. [3]

2.2 Transverse Young's Modulus $E_\perp$

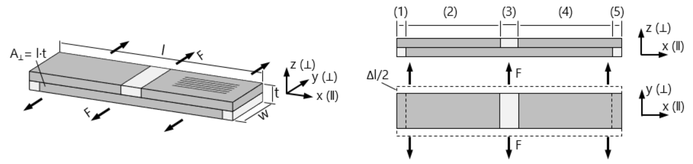

Figure 4: Representative unit cell of FPP lamina with uniaxial loading transverse to fiber direction.

Transverse Young's modulus of the unit cell the requires parallel connection of sections (1) to (5):

Equilibrium of forces: $F_\perp = \Sigma F_i$ or $\sigma_\perp \cdot A_\perp = \Sigma \sigma_i \cdot A_i$; $i = (1), (2), (3), (4), (5)$

Kinematic relations: $\varepsilon_\perp = \varepsilon_i$

Geometrical relations: $A_\perp = \Sigma A_i$; $A_{(2)} = A_{(4)} \Rightarrow A_{patch} = 2A_{(2)}$
$A_{(3)} = A_{(1)} + A_{(5)} \Rightarrow A_{gap} = 2A_{(3)}$

Law of elasticity: $\sigma_{(2)} = \sigma_{(4)} = E_{(2)} \cdot \varepsilon_{(2)}$ (patch sections)
$\sigma_{(3)} = \sigma_{(1)} + \sigma_{(5)} = E_{(3)} \cdot \varepsilon_{(3)}$ (butt joint sections)
$\Rightarrow E_\perp \varepsilon_\perp A_\perp = E_{(2)} \varepsilon_{(2)} 2A_{(2)} + E_{(3)} \varepsilon_{(3)} 2A_{(3)}$
$\varepsilon_\perp = \varepsilon_i \Rightarrow E_\perp A_\perp = E_{(2)} 2A_{(2)} + E_{(3)} 2A_{(3)}$
$\Rightarrow E_\perp = \frac{2A_{(2)}}{A_\perp} \cdot E_{(2)} + \frac{2A_{(3)}}{A_\perp} \cdot E_{(3)}$

Assumptions made: $\frac{2A_{(2)}}{A_\perp} \approx 1$ (patch sections) ; $\frac{2A_{(3)}}{A_\perp} \approx 0$ (butt joint sections)

$\Rightarrow E_\perp = E_{(2)} = E_{patch}$. The transverse Young's modulus of the FPP lamina is equivalent to the continuous fiber-reinforced composite.

3 Tensile Strength and Failure of FPP laminae

Due to the discontinuous fiber architecture the tensile strength of FPP laminates has to be lower than for classic laminates. According to HORN's work it is about 52–57 % of continuous unidirectional (UD) fiber-reinforced composites. This phenomenon can be explained by the critical spot of a FPP structure, the butt joint of two patches. Tensile load in fiber direction x(1) causes normal stress σ_1 and shear stress τ_{13} at the patch ends. The tensile strength in the butt joint cross-section is estimated according to: $R_{FPP} = (R_{patch} + R_{matrix})/2$, resulting in a strength of the FPP laminate of slightly more than 50 % of the classic laminate. Of course, the tensile strength of the patches is not exhausted yet, which implies that the shear strength limit S_{13} at the patch end is already reached at this load, causing the laminate to fail. An analytical comparison of the tensile strength between a continuous UD-reinforced composite lamina and a structural FPP lamina is displayed in Figure 5. The material used is a common carbon fiber / epoxy composite IM7 / 8552 (fiber volume content = 60 %). [6] The patch length of the FPP lamina is 60 mm with an each-other overlap of 50 % (see Figure 2). Both laminae are exposed to uniaxial tensile load. Influence of shear stress is considered by a linear correlation between τ_{13} and σ_1.

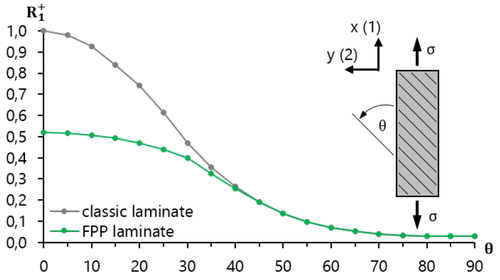

$$\left(\frac{\sigma_1}{R_1^+}\right)^2 + \left(\frac{\tau_{12}}{S_{12}^+}\right)^2 + \left(\frac{\tau_{13}}{S_{13}^+}\right)^2 = 1$$

Longitudinal fiber tensile failure

$$\left(\frac{\sigma_2}{R_2^+}\right)^2 + \left(\frac{\tau_{12}}{S_{12}^+}\right)^2 + \left(\frac{\tau_{13}}{S_{13}^+}\right)^2 = 1$$

Transverse fiber tensile failure

Figure 5: Tensile strength of unidirectional CFRP laminae as a function of the fiber orientation / off-axis angle θ.

The stresses have been calculated with Classical Laminate Theory (CLT) and the strength was determined by HASHINS' failure criteria for tensile load. [7] Due to varying off-axis angle both longitudinal (fiber-dominant) and transverse (matrix-dominant) failure mode have to be checked simultaneously. From an off-axis angle $\theta \geq 40°$ the difference in tensile strength between classic and FPP composites vanishes. This agrees well with the work of HORN in terms of tendency. [3]

4 Conclusion and Outlook

Comprehensive development of structural mechanics of patch-based composites on a reduced and simplified level sets the foundation for further investigations. This work shall complement the existing research on FPP laminates with regard to analytical description of fundamental engineering constants. Next step is to setup a simulation model according to test standard requirements in order to perform virtual tensile tests of FPP laminate specimen with defined patch lay-up and overlap pattern. Experimental test series will be conducted to obtain material parameters (strengths, strains) in order to calibrate simulation and review analytics for validity (e.g. DIN EN 2561, DIN EN 2597).

References

[1] N. N.: *CEVOTEC - FPP Technology.* www.cevotec.com/fpp-technologie, December 2019

[2] MEYER, O.: *Kurzfaser-Preform-Technologie zur kraftflussgerechten Herstellung von Faserverbundbauteilen.* Dissertation, Universität Stuttgart, 2008

[3] HORN, B.: *Beitrag zum Materialverständnis von langfaserpatch-verstärkten Bauteilen.* Dissertation, Technische Universität München, 2018

[4] KUSSMAUL, R.: *Design and Optimization of Variable Stiffness Composites Structures from Patched Laminates.* Dissertation, Eidgenössische Technische Hochschule Zürich, 2019

[5] SCHÜRMANN, H.: *Konstruieren mit Faser-Kunststoff-Verbunden.* Springer-Verlag, Berlin / Heidelberg / New York, 2007

[6] KADDOUR, A. S.; ET AL: *Mechanical properties and details of composite laminates for the test cases used in the third world-wide failure exercise.* Journal of Composite Materials, Volume 47, 2013

[7] FLEMMING, M.; ROTH, S.: *Faserverbundbauweisen - Eigenschaften / mechanische, konstruktive, thermische, elektrische, ökologische, wirtschaftliche Aspekte.* Springer-Verlag, Berlin / Heidelberg, 2003

Contact

Andreas Baumer, M.Sc.
Research assistant / PhD student
Composite Technology & Lightweight Design
T +49 821 5586 3664
andreas.baumer@hs-augsburg.de

Augsburg University of Applied Sciences
Faculty of Mechanical and Process Engineering
An der Hochschule 1
86161 Augsburg
www.hs-augsburg.de